Supporting Information

Targeting mitochondrial DNA with a two-photon active Ru(II) phenanthroline derivative

Hui Wang[a†], Xiaohe Tian[b†], Lijuan Guan[c], Qiong Zhang[a], Shengyi Zhang[a], Hongping Zhou[a], Jieying Wu*[a], Yupeng Tian*[a,d]

† *These authors contributed equally to this work.*

[a] Department of Chemistry, Key Laboratory of Functional Inorganic Material Chemistry of Anhui Province, Anhui University, Hefei 230601, P. R. China;

[b] School of Life Science, Anhui University, Hefei 230601, P.R. China

[c] Department of Chemistry, University College London, WC1H0AJ, UK

[d] State Key Laboratory of Coordination Chemistry, Nanjing University, Nanjing 210093, P. R. China

**Corresponding author. Tel: +86-551-63861227*

E-mail address: jywu1957@163.com; yptian@ahu.edu.cn

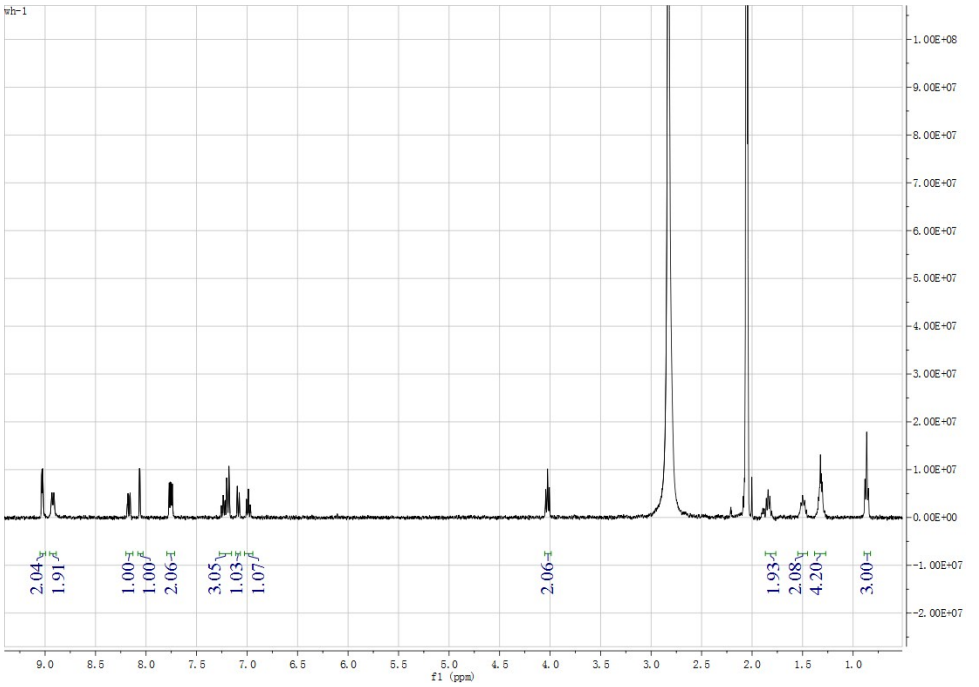

Fig S1. ^{1}H NMR spectra of **HL**.

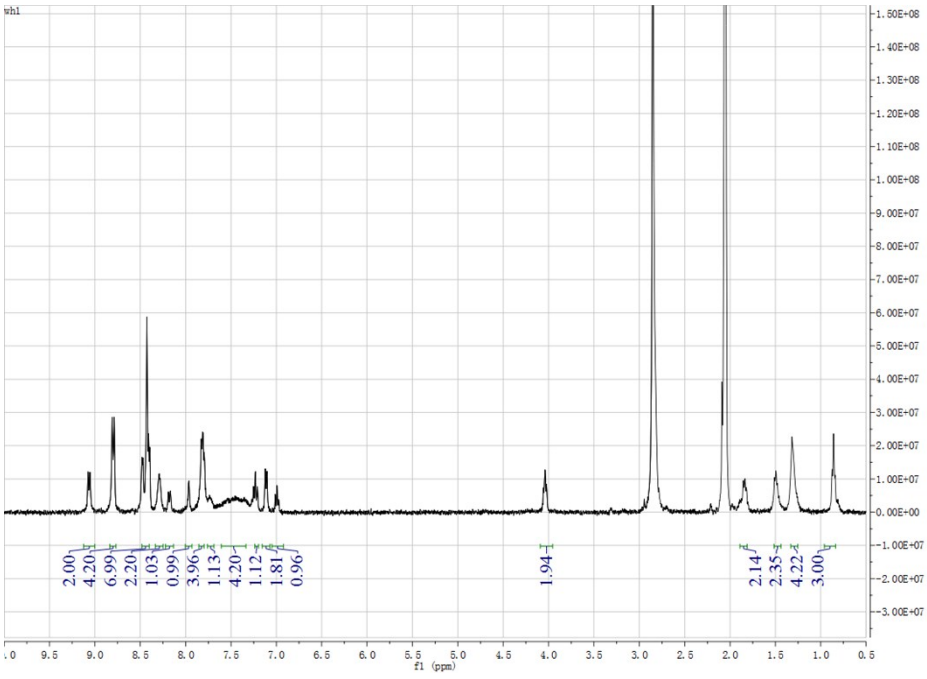

Fig S2. ^{1}H NMR spectra of **HLRu**.

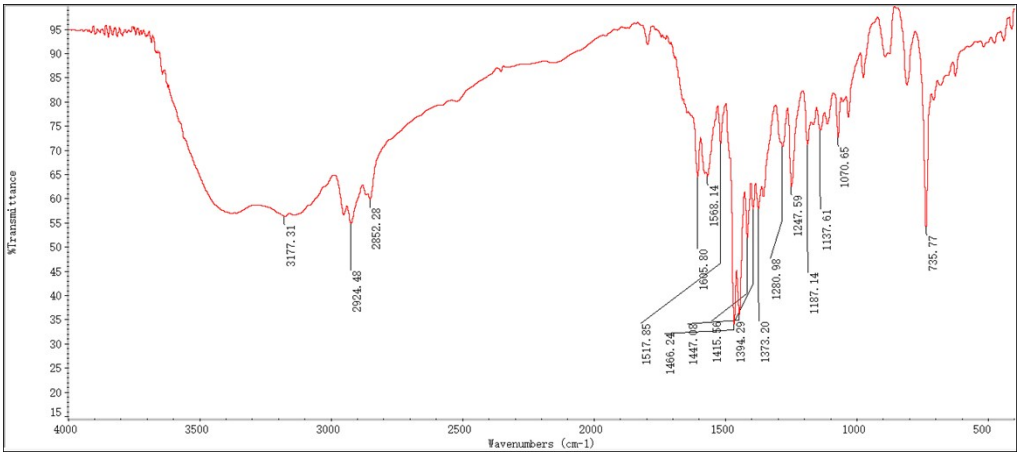

Fig S3. IR spectra of **HL**.

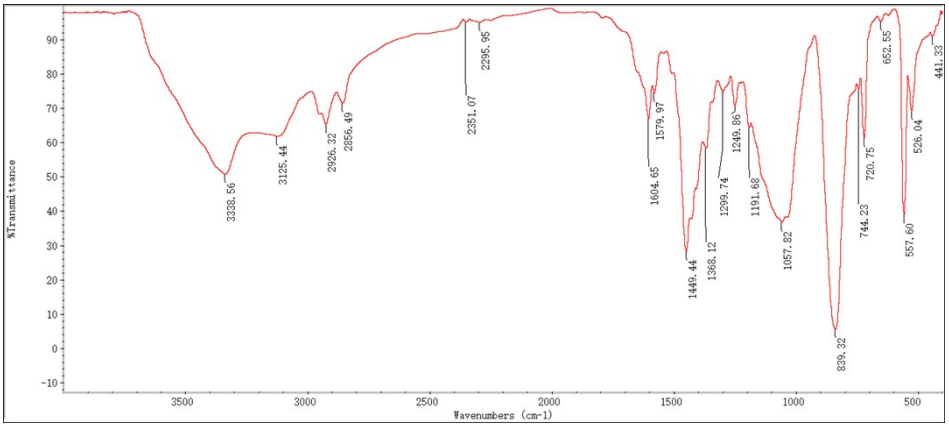

Fig S4. IR spectra of **HLRu**.

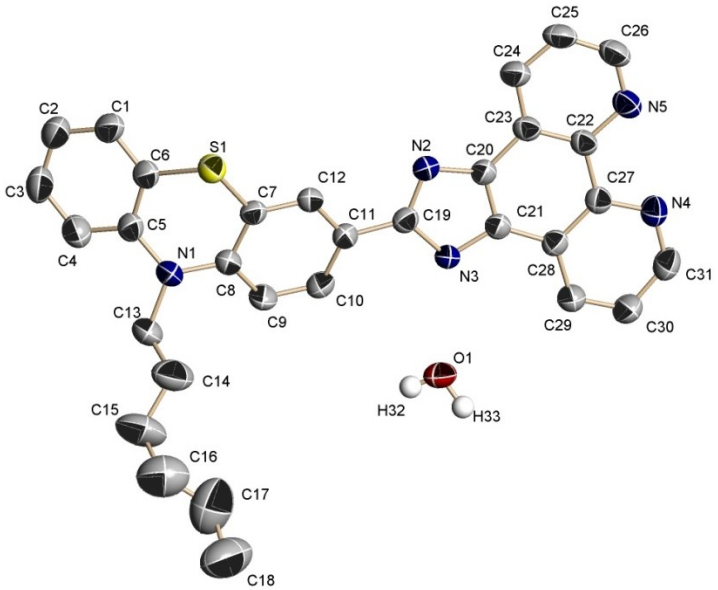

Fig S5. Crystal structure of **HL**, all H atoms were omitted for clarity.

Table S1. Crystal data collection and structure refinement of **HL**

Compound	**HL**
Empirical formula	$C_{31}H_{29}N_5OS$

Formula weight	519.65
Crystal system, space group	Monoclinic, $P2_1/c$
Unit cell dimensions(Å,)	a=12.507(5)
	b=16.431(5)
	c=13.315(5)
	β=108.61(5)
Volume/ $Å^3$	2593(2)
Z, Calculated density/Mg m^3	4, 1.331
Absorption coefficient/mm^{-1}	0.160
F(000)	1096
Theta range for data collection/	1.72 to 24.99
Completeness to theta=24.99	99.8%
Goodness-of-fit on F^2	0.965
Final R indices [I>2σ]	R_1=0.0525, wR_2=0.1447
Large diff. peak and hole/e $Å^{-3}$	0.484and -0.304

Table S2. Selected bond lengths (Å) and angles (°) of **HL**

HL			
N(4)-C(31)	1.325(4)	C(22)-N(5)	1.358(3)
N(4)-C(27)	1.356(5)	C(6)-S(1)-C(7)	98.0(1)
C(31)-N(4)-C(27)	117.1(2)	N(2)-C(19)-N(3	112.1(2)

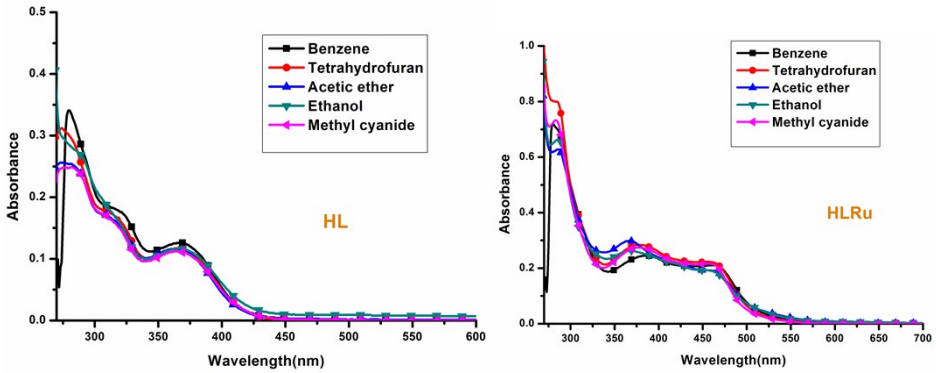

Fig S6. Linear absorption spectra of **HL** and its **Ru(II)** complex in different solvents($c=1.0\times10^{-5}$ mol/L).

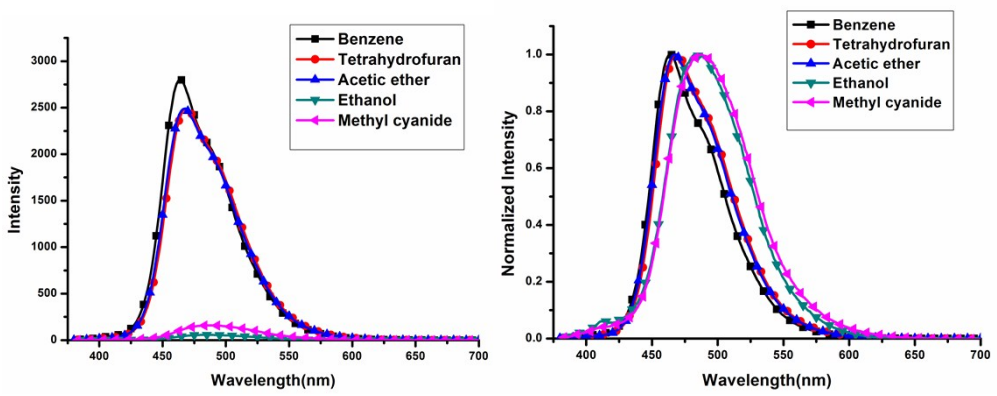

HL

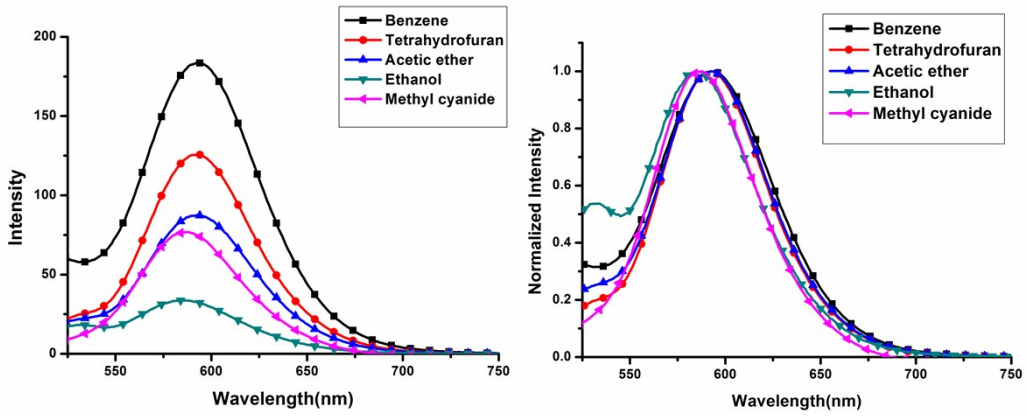

HLRu

Fig S7. Single-photon excited fluorescence spectra of **HL** and complex **HLRu** in different solvents (c=1.0×10^{-5} mol/L).

Table S3. The photophysical data of **HL** and complex **HLRu** in different solvents.

Compound	Solvents	λ_{max}^{abs} (nm)[a]	logε$_{max}$	λ_{max}^{SPEF} (nm)[b]	τ[c]	Δν (cm^{-1})[d]
HL	Benzene	365	4.10	464	3.84	5845
	Tetrhydrofuran	363	4.07	468	3.45	6180
	Ethanol	364	4.07	483	0.16	6768
	Ethyl acetate	360	4.06	468	4.15	6410
	Acetonitrile	363	4.05	488	0.50	7056
HLRu	Benzene	458	4.32	593	71.6	4971
	Tetrhydrofuran	456	4.32	593	95.8	5066
	Ethanol	457	4.31	593	97.4	5018

Ethyl acetate	456	4.32	585	110	4835
Acetonitrile	456	4.31	587	71.7	4894

[a] Peak position of the longest absorption band. [b] Peak position of SPEF, excited at the absorption maximum. [c] Fluorescence lifetime (ns). [d] stokes' shift in cm^{-1}

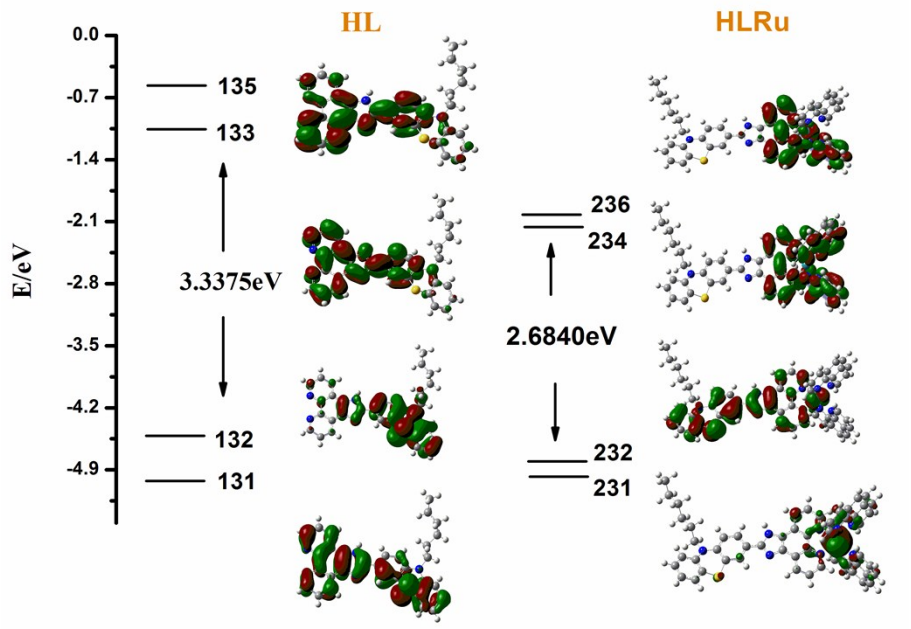

Fig S8. Molecular orbital energy diagram for **HL** and **HLRu**.

Table S4. Calculated leaner absorption properties (nm), excitation energy (eV), oscillator strengths and major contribution for **HL** and complex **HLRu**.

Cmpd	ΔE_1[a]	λ[nm][b]	Oscillator strengths	Nature of the transition
HL	3.34	371	0.32	132(H)→133(L)(0.65)
	4.00	309	0.17	131(H-1)→133(L)(0.49)
	4.43	280	0.11	131(H-1)→135(L+2)(0.54)
HLRu	2.71	458	0.001	231(H-2)→234(L)(0.49)
	3.33	372	0.014	232(H-1)→236(L+2)(0.40)

[a] The energy gap of the single-photon absorption band. [b] Peak position of the maximum absorption band.

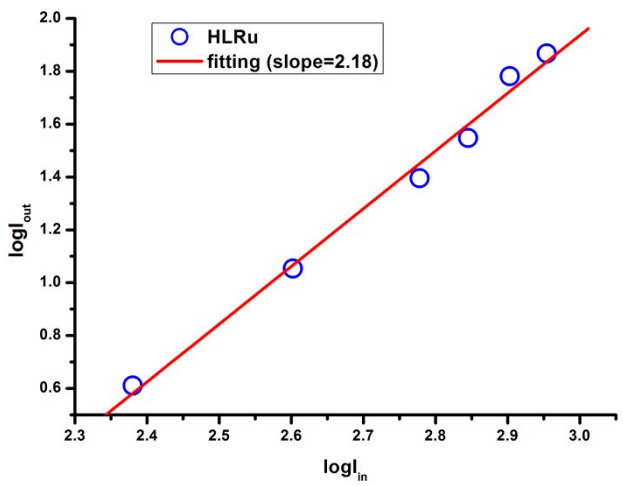

Fig S9. Output fluorescence (I_{out}) vs. the square of input laser power (I_{in}) for **HLRu**.

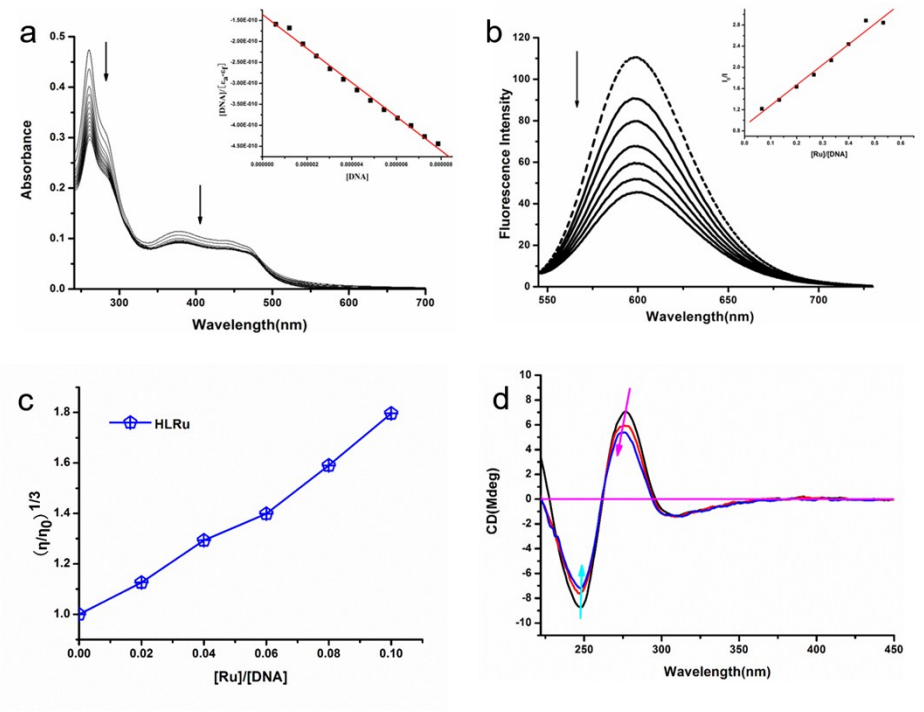

Fig S10. (a) UV-vis absorption spectra of **HLRu** (10 μM), in the absence and presence of increasing concentrations of ct-DNA (0-8 μM) in 50 mM Tris-HCl buffer (pH=7.4, 50 mM NaCl). Inset: plots of [DNA]/(ε_a-ε_f) vs. [DNA] and the linear fit line. (b) Fluorescence spectra of EB bound to DNA in the presence of **HLRu** (0 - 27 μM). [EB] = 50 μM, [DNA] = 50 μM. The arrows show the intensity changes upon increasing concentrations of the complex. Inset: florescence quenching curve of DNA-bound EB by **HLRu**. (c) The changes in the relative viscosities of DNA with increasing concentrations of **HLRu** in buffer 50 mM NaCl. The total concentration of DNA is 0.24 mM. (d) Circular dichroism spectra of ct-DNA in the absence (DNA alone) and presence of **HLRu**.

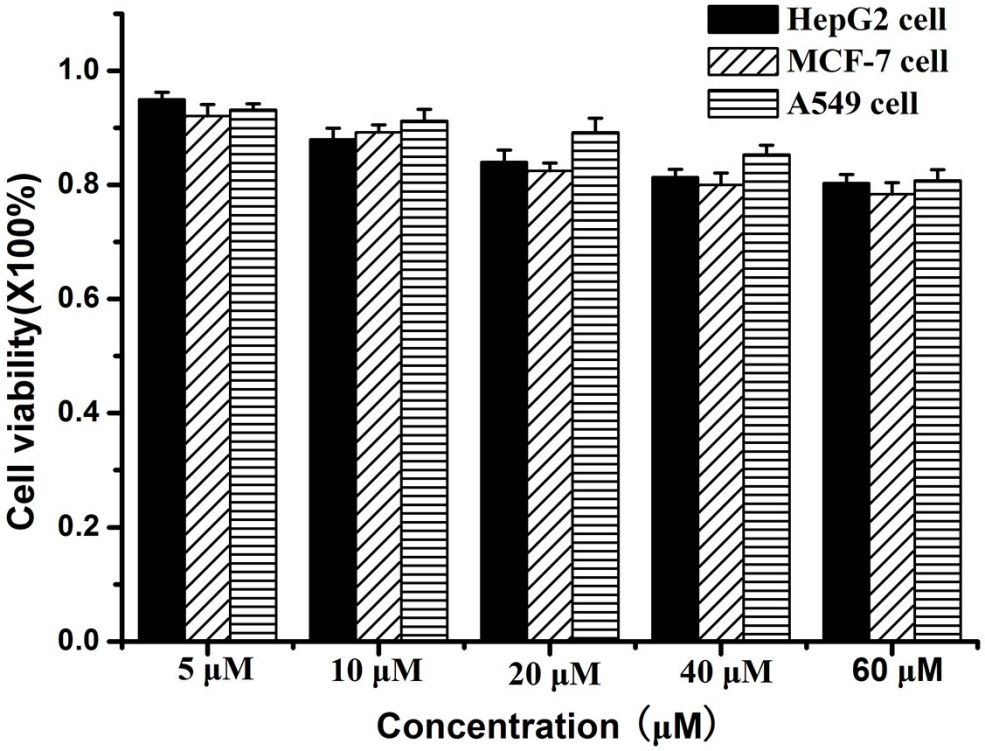

Fig S11. Cytotoxicity data results obtained from the MTT assay.

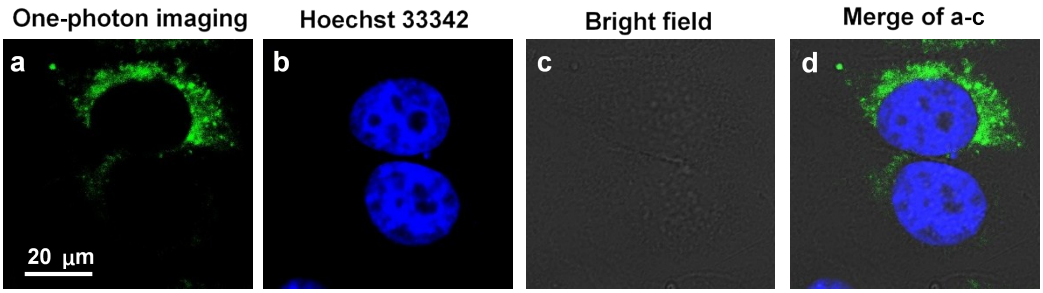

Fig S12. One-photon image of HepG2 live cells incubated with **HLRu** co-staining with Hoechst 33342 excited in maximum of absorption wavelength and the fluorescence emission measured at 570-600 nm and 410-440 nm.

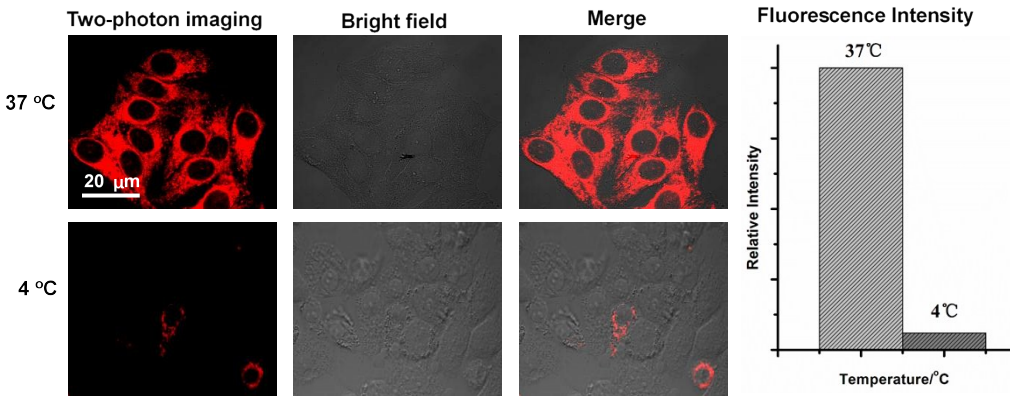

Fig S13. Two-photon image of HepG2 cells incubated with complex **HLRu** at 37 °C and 4 °C for

30 minutes.

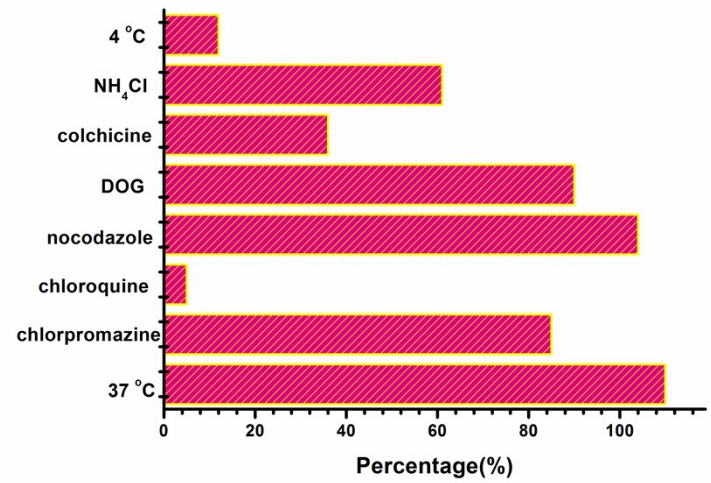

Fig S14. Endocytosis inhibition of **HLRu** in HepG2 cells using various endocytosis inhibitors.

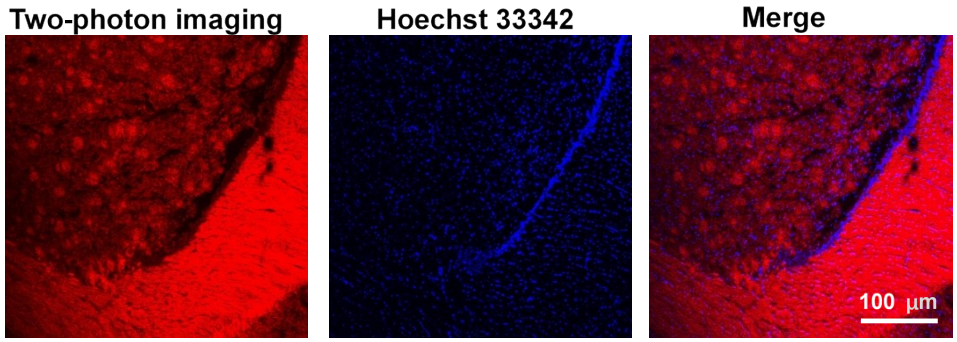

Fig S15. Two-photon fluorescence images of a fresh mouse brain slice incubated with **HLRu** and then further incubated with Hoechst 33342 at depths of approximately 0-100 μm.